



ORIGINAL PAPER

PREDICTION OF BOND WORK INDEX AND HARDGROVE GRINDABILITY INDEX VALUES FROM MECHANICAL AND INDEX TESTS USING DEEP NEURAL NETWORKS METHOD**Halil BÖLÜK¹⁾, *, Çağrı ALDI²⁾ and Olgay YARALI³⁾**¹⁾ Department of Mining and Mineral Extraction, Caycuma Vocational School, Zonguldak Bulent Ecevit University, Zonguldak, Turkey²⁾ Department of Mining and Mineral Extraction, Caycuma Vocational School, Zonguldak Bulent Ecevit University, Zonguldak, Turkey³⁾ Department of Mining Engineering, Faculty of Engineering, Zonguldak Bulent Ecevit University*Corresponding author's e-mail: halil.boluk@beun.edu.tr**ARTICLE INFO****Article history:**

Received 17 September 2025

Accepted 15 December 2025

Available online 12 January 2026

Keywords:

Deep Neural Networks (DNN)

Bond Work Index (BWI)

Hardgrove Grindability Index (HGI)

Rock mechanics

Grindability prediction

ABSTRACT

Prediction of the Bond Work Index (BWI) and Hardgrove Grindability Index (HGI) from routinely measured rock mechanical and index parameters is critical for energy-efficient comminution design, yet remains challenging due to complex, nonlinear relationships among strength, abrasivity and energy consumption. This study proposes a deep neural network (DNN)-based machine-learning framework to estimate BWI and HGI using mechanical and index test results obtained from 24 coal surrounding rock samples (sandstone and siltstone) from the Zonguldak Basin.

The input space is constructed from seven routinely performed laboratory tests describing rock strength, drillability, abrasivity and hardness. Correlation analysis and Variance Inflation Factor (VIF)-based screening are employed to identify and remove redundant or weakly contributing parameters, leading to more compact DNN architectures. The resulting models achieve high predictive performance, with R^2 values of about 0.8–0.86 for BWI and up to about 0.95–0.96 for HGI on the available dataset and additional stratified train–test splits and cross-validation analyses confirm the potential of the approach, particularly for HGI prediction.

Overall, the proposed methodology demonstrates that DNNs can capture multi-parameter nonlinear interactions more effectively than traditional empirical formulations and offers a practical tool for rapid grindability assessment, mining energy optimization and the development of data-driven rock characterization workflows.

INTRODUCTION

In underground mining operations, the selection and performance prediction of mechanized excavation machines (such as roadheaders and electro-hydraulic drills) are key factors for economically efficient gallery development. A central component of this problem is the assessment of rock breakage and grinding behaviour, since grinding strongly influences both energy consumption and overall process efficiency. The close coupling between excavation method selection and geological conditions has been demonstrated in several case studies, for example along the Black Sea Coastal Road, where the tunnelling method was systematically related to the local geological structure (Külekci, 2022).

Grinding operations are among the most energy-intensive stages in mineral processing, often accounting for 50–70 % of the total energy consumption in mining operations (Ballantyne and Powell, 2014). The success of improving grinding efficiency is therefore measured primarily by reductions in specific energy consumption, while achieving the required particle size distribution at the lowest possible energy cost per ton of processed material. With the depletion of high-grade mineral

deposits and the transition toward low-grade but large-scale ore bodies, the importance of grinding has further increased, particularly in relation to mineral liberation and downstream recovery (Oner, 1983). Determining grindability characteristics is thus essential for designing efficient grinding circuits, selecting appropriate equipment and optimizing operating parameters to meet product specifications while minimizing energy and operating costs.

Another important consideration in grinding circuits is the control of excessive fines production, which can increase processing costs and adversely affect product quality. Accordingly, understanding and predicting the particle size distribution of ground material is crucial for process control and optimization, and plays a vital role in ensuring both energy savings and stable plant performance. Related studies on rock-like and cementitious materials have highlighted the importance of linking experimental measurements with predictive frameworks to better understand material response under different conditions, such as in investigations of fly ash-added lightweight concretes and their gamma radiation transmission properties (Külekci, 2021).

Grindability has been extensively studied over the years, with a large proportion of the work focusing on coal, whereas studies on the grindability of other rock types remain relatively limited (Aldi, 2023). Among grindability test methods, the Hardgrove Grindability Index (HGI) is widely used due to its simplicity and practicality in both research and industry (Berry and Bruce, 1966; Horst and Bassarear, 1976; Karra, 1981; Magdalinović, 1989). Bond (1954, 1961) examined the relationship between HGI and the Bond Work Index (BWI) for coals, and subsequent studies adapted Bond's approach to limestone and other brittle materials (Haese et al., 1975; McIntyre and Plitt, 1980). Similar empirical relationships have been proposed for bauxite (Csöke et al., 2004) and carbonate rocks (Hower et al., 1992), underscoring the close relationship between HGI, BWI and rock breakage behaviour.

A number of researchers have investigated correlations between grindability indices and various mechanical or index properties of rocks. These efforts include comparisons of different grindability determination methods (Ersayin and Kirsan, 1995), correlations between hardness properties and HGI for coal deposits (Tiryaki et al., 2001; Tiryaki, 2005), and studies linking HGI to uniaxial compressive strength and Shore hardness in Zonguldak bituminous coals (Su et al., 2004). Swain and Rao (2009) reported strong linear correlations between HGI-derived and experimentally determined BWI values for several rock types, demonstrating that HGI can be a practical indicator of rock grindability. Other works have evaluated relationships between BWI and physico-mechanical parameters such as ultrasonic velocity, Shore hardness, point load index and uniaxial compressive strength, and emphasized the need for further studies to generalize these findings (Sengun et al., 2006; Ozer and Cabuk, 2007). Additional investigations have reported exponential relationships between BWI and uniaxial compressive strength (Abdelhaffez, 2012) and linked tensile strength and BWI to drilling penetration rates (Park and Kim, 2020).

More recently, data-driven models have been introduced to better capture the complex interactions controlling grindability. Aras et al. (2020) used artificial neural networks (ANN) to predict BWI from rock properties such as Schmidt hardness, uniaxial compressive strength, Brazilian tensile strength, point load index, ultrasonic velocity and density, achieving R^2 values between 0.85 and 0.91 and demonstrating the potential of machine-learning-based approaches. Sakiz (2021a) showed that the Drilling Rate Index (DRI) could be estimated from HGI for a limited rock set, and later investigated the relationship between abrasiveness and grindability in andesitic rocks using HGI and different abrasivity tests (Sakiz, 2021b). In parallel, Cerchar Abrasivity Index (CAI) variability has been analysed statistically for different rock types, providing a broader context for understanding CAI behaviour and its implications for tool wear and rock–

tool interaction (Külekcı and Yurtsever, 2025). Complementary advances in deep learning have also enhanced mineral processing workflows, for example through automated quartz identification from thin section images using convolutional neural networks (Külekcı et al., 2025), illustrating the potential of modern AI methods in mineralogical and textural characterization.

Despite these advances, there is still a clear need for predictive frameworks that explicitly account for the complex, nonlinear and multi-parameter interactions governing grindability, while also addressing multicollinearity among input variables. Most existing empirical, regression and ANN-based models are built on relatively small datasets, do not systematically combine feature selection with advanced nonlinear modelling, and are rarely evaluated using multiple validation strategies, which limits their generalizability.

In this context, the present study aims to develop a Deep Neural Network (DNN)-based machine-learning model for predicting both BWI and HGI from routinely measured mechanical and index parameters of coal surrounding rocks from the Zonguldak Basin. The central hypothesis is that DNNs, when combined with correlation and Variance Inflation Factor (VIF)-based feature selection, can provide higher predictive accuracy and a clearer assessment of parameter sensitivity than conventional empirical, regression and ANN models, even for relatively small datasets.

The specific contributions of this work are: (i) to construct and evaluate DNN models for BWI and HGI prediction using a consistent experimental dataset of sandstone and siltstone samples; (ii) to systematically optimize the input parameter set through correlation and VIF analysis in order to enhance model interpretability and generalization; and (iii) to benchmark the obtained prediction performance against values reported in previous grindability studies, including additional cross-validation schemes, thereby clarifying the added value and limitations of the proposed DNN-based approach.

MATERIALS AND METHODS

ROCK SAMPLING AND LABORATORY TESTING

In this study, mechanical and index tests were conducted on 24 coal surrounding rock samples (sandstone and siltstone) obtained from active underground mining areas in the Zonguldak Basin. Sampling and specimen preparation followed ISRM (1978, 1981, 2007) recommendations, ensuring that all cores and blocks were representative and suitable for the planned tests. The tested parameters include uniaxial compressive strength (σ_c), Brazilian tensile strength (σ_t), Sievers' J-miniature drill test (SJ), brittleness test (S20), Drilling Rate Index (DRI), Cerchar Abrasivity Index (CAI), Equotip Hardness Index (ESD), as well as Hardgrove Grindability Index (HGI) and Bond Work Index (BWI). Descriptive statistics for all variables are summarized in Table 1.

Table 1 Statistical summary of rock parameters.

Parameter	Unit	Mean	Std Dev	N
σ_c	MPa	45.2	18.7	24
σ_t	MPa	3.8	1.6	24
SJ	-	28.5	12.3	24
S20	-	42.1	15.8	24
DRI	-	35.7	14.2	24
CAI	-	2.8	0.9	24
ESD	-	485	125	24
BWI	kWh/t	17.0	2.5	24
HGI	-	86.0	14.0	24

All laboratory tests were performed in controlled conditions using standard or widely accepted procedures. The main devices used in this study are illustrated in Figure 1, including the Hardgrove mill, Bond ball mill, hydraulic press, brittleness and miniature drill test setups, CAI test equipment, microscope imaging system and Equotip hardness tester.

The Hardgrove Grindability Index (HGI) was determined using the standard Hardgrove test, which quantifies the mass of material passing 75 μm after grinding under fixed conditions in a standardized laboratory mill (Hardgrove, 1932). The procedure follows the classical protocol: a fixed mass of material within a specified feed size range is ground in a steel grinding bowl containing steel balls under a defined normal load and number of revolutions (Fig. 1a). After grinding, the mass passing 75 μm is measured and converted to HGI using the calibration chart for the tested material.

HGI values were calculated using the classical expression Eq. 1.

$$\text{HGI} = 13 + 6.93D \quad (1)$$

where

HGI is the Hardgrove Grindability Index, and D is the mass of material (g) passing through the 200 (75 μm) sieve under the standard test conditions.

The Bond Work Index (BWI) was determined using the standard Bond ball mill grindability test, which is a closed-circuit dry grinding and screening procedure conducted under fixed mill dimensions, ball charge, rotational speed and test sieve size (Bond, 1954; Bond, 1961; Deniz, 1996). The test aims to reach a steady-state circulating load (typically 250 %) by repeatedly grinding and screening the material until equilibrium is achieved between fresh feed and ground product.

A standard Bond mill with internal dimensions of 305 \times 305 mm, a specified ball charge and fixed rotational speed was used (Fig. 1b). The material was prepared to the prescribed feed size and subjected to repeated grinding cycles. For each cycle, the mass of material passing the test sieve was recorded, and the net grindability value (G_{bg} , g/rev) was obtained from the mass of newly produced undersize per revolution. After steady-state conditions were reached, the BWI (kWh/t) was calculated using the classical Bond Eq. 2.

$$\text{BWI} = \frac{1.1 \times 44.5}{(P_1^{0.23} G_{bg}^{0.82} (\frac{10}{\sqrt{P}} - \frac{10}{\sqrt{F}}))} \quad (2)$$

Where

BWI is the Bond Work Index (kWh/t), P_1 is the aperture size of the test sieve (μm), G_{bg} is the Bond standard ball mill grindability (g/rev),

P is the 80 % passing size of the product (μm), F is the 80 % passing size of the feed (μm).

Rock strength was characterized using uniaxial compressive strength (σ_c) and Brazilian tensile strength (σ_t) tests. The ISRM (1981) suggested method was followed for UCS, using right-cylindrical specimens with appropriate slenderness and end preparation. Brazilian tensile strength tests followed ISRM (1978) guidelines using disc-shaped specimens loaded along their diameter until failure. Both tests were carried out on a servo-controlled hydraulic press (Fig. 1c), and σ_c and σ_t were computed from the peak loads and specimen geometries.

The drillability of the rocks was assessed using the brittleness index (S20) and Sievers' J-miniature drill test (SJ). The S20 test quantifies the amount of material passing a given sieve after a standardized impact sequence, whereas the SJ test measures the depth of penetration of a miniature drill bit under fixed load and rotational speed. The corresponding apparatus are shown in Figures 1d and 1e.

The Drilling Rate Index (DRI) was then calculated from SJ and S20 values using the standard chart proposed by Dahl (2003), which relates brittleness and drillability to a dimensionless DRI value (Fig. 2).

Rock abrasiveness was evaluated using the Cerchar Abrasivity Index (CAI). The tests were conducted following the procedure described by Alber et al. (2013), in which a hardened steel stylus is drawn across a rock surface under constant load and the resulting wear flat diameter is measured. The automatic CAI testing device used in this study is shown in Figure 1f, while the computer-assisted microscope and imaging system used to measure the wear flats are illustrated in Figure 1g. Typical measurements of worn stylus tips in horizontal and vertical orientations are presented in Figure 3.

Rock surface hardness (ESD) was determined using a portable Equotip hardness tester (type D),

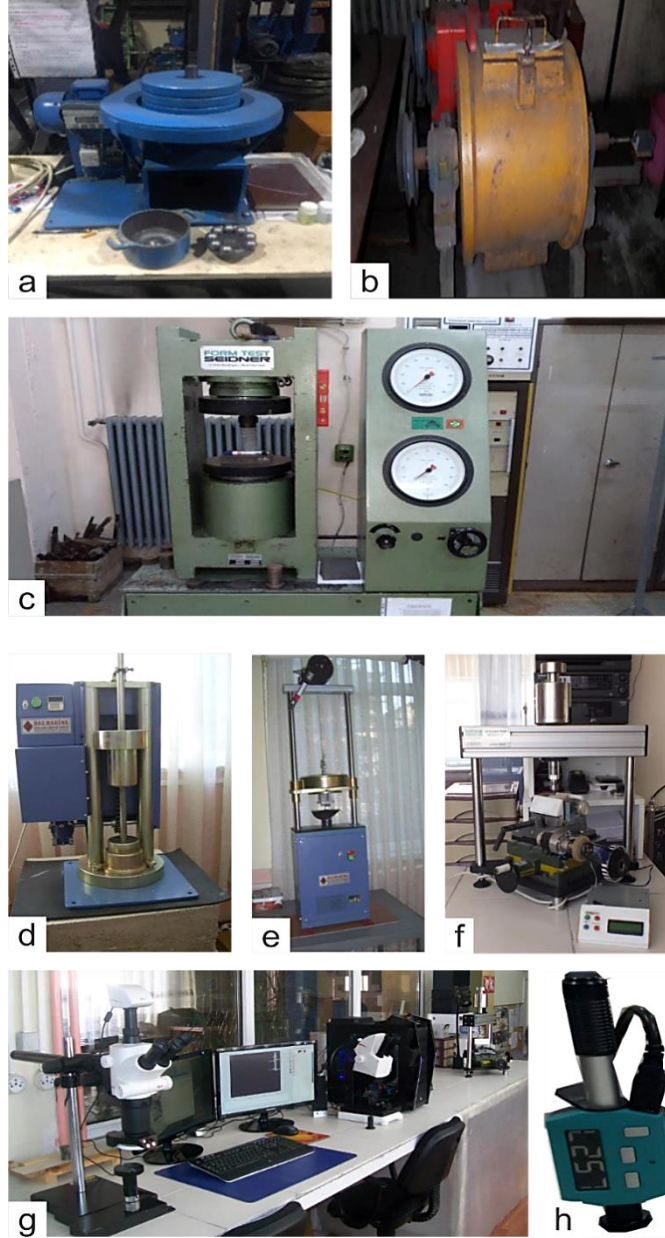


Fig. 1 All test apparatus and devices used in this study. a) Hardgrove Grindability Index (HGI) test apparatus. b) Bond ball mill test apparatus. c) Hydraulic press used for the strength tests. d) S20 brittleness test apparatus. e) Sievers J miniature test apparatus. f) West fully automatic CAI testing apparatus. g) Imaging system using a computer-assisted microscope. h) Equotip hardness tester used in the study.

which employs a tungsten carbide impact body and measures the rebound velocity to compute a dimensionless hardness index (Fig. 1h). In this study, multiple Equotip readings were taken on each specimen and averaged to obtain the ESD value used as an input parameter in the subsequent modelling steps.

DATA PREPROCESSING AND DNN MODELLING

For the machine-learning analysis, two separate prediction problems were defined with BWI and HGI as the target variables. In both cases, the same set of seven routinely measured rock parameters was used as input features: $\{\sigma_c, \sigma_t, SJ, S20, DRI, CAI, ESD\}$.

The resulting dataset consists of 24 samples and 7 input variables. Prior to model training, all input variables were standardized to zero mean and unit variance using z-score normalization. For each feature x_j , the normalized value x'_{ij} of sample i is defined as Eq. 3:

$$x'_{ij} = \frac{x_{ij} - \mu_j}{\sigma_j} \quad (3)$$

where μ_j and σ_j are the mean and standard deviation of feature j computed from the training set only. The same scaling parameters were applied to the test data to avoid information leakage. Normalization was implemented in Python using the Standard Scaler utility from scikit-learn.

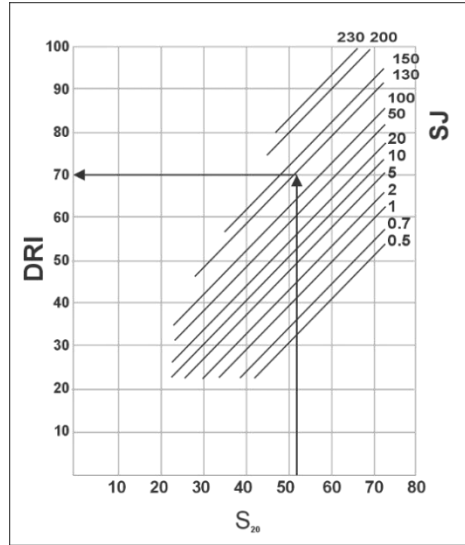


Fig. 2 Diagram used for determining the DRI (Dahl, 2003).

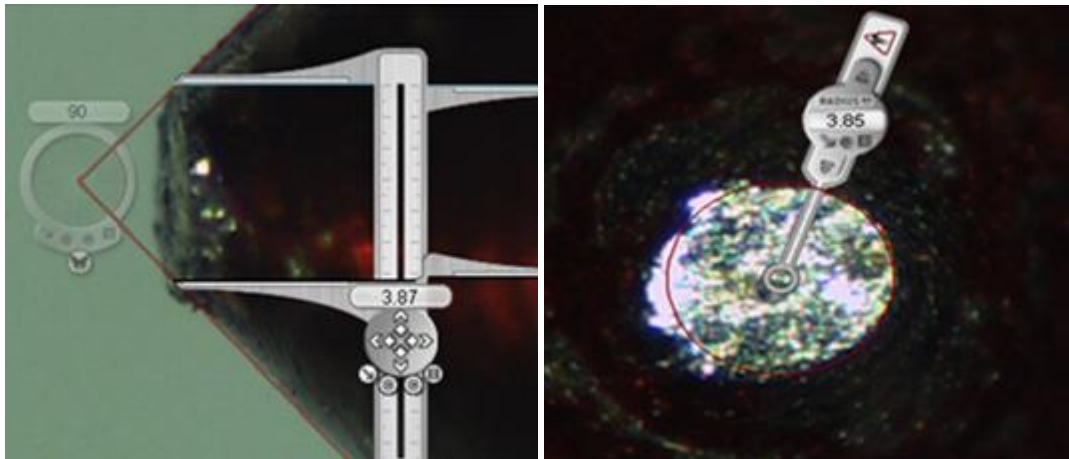


Fig. 3 Measurement of worn tips in horizontal and vertical positions under the microscope.

To reduce redundancy and mitigate multicollinearity, a correlation analysis and Variance Inflation Factor (VIF) screening were carried out before finalizing the DNN input sets. Pearson correlation coefficients between all mechanical/index parameters and the grindability indices (BWI, HGI) were computed, and the full correlation matrix is shown in Figure 4.

VIF values were then calculated for each input variable based on a multiple linear regression framework. Variables with $VIF > 5$ were considered to exhibit problematic multicollinearity and were examined for possible removal, together with parameters showing weak physical relevance to grindability. Several candidate subsets were evaluated by training DNN models with different combinations of input variables. This procedure resulted in optimized feature sets for BWI and HGI prediction, which are discussed in detail in the Results and Discussion section.

Deep Neural Networks (DNNs) were used to model the nonlinear relationships between the rock parameters and the grindability indices. The networks

were implemented in Python using the TensorFlow/Keras framework (Goodfellow et al., 2016). Each model consisted of an input layer with 7 neurons (one for each normalized feature), four fully connected hidden layers and a single-neuron output layer for regression. The final architecture adopted in this study is summarized in Table 2.

Hidden layers contained 64, 32, 16 and 8 neurons, respectively, and used the Swish activation function, which has been shown to perform well in deep networks with complex nonlinear interactions (Ramachandran et al., 2017). The output layer used a linear activation to predict continuous BWI or HGI values. A summary of the main hyperparameters (learning rate, batch size, maximum epochs, optimizer, loss function and validation split) is given in Table 3.

Model training was performed using the mean squared error (MSE) as the loss function and Stochastic Gradient Descent (SGD) as the optimizer, with a learning rate of 0.001 and a mini-batch size of 8. To prevent overfitting, early stopping was employed: training was terminated if the validation

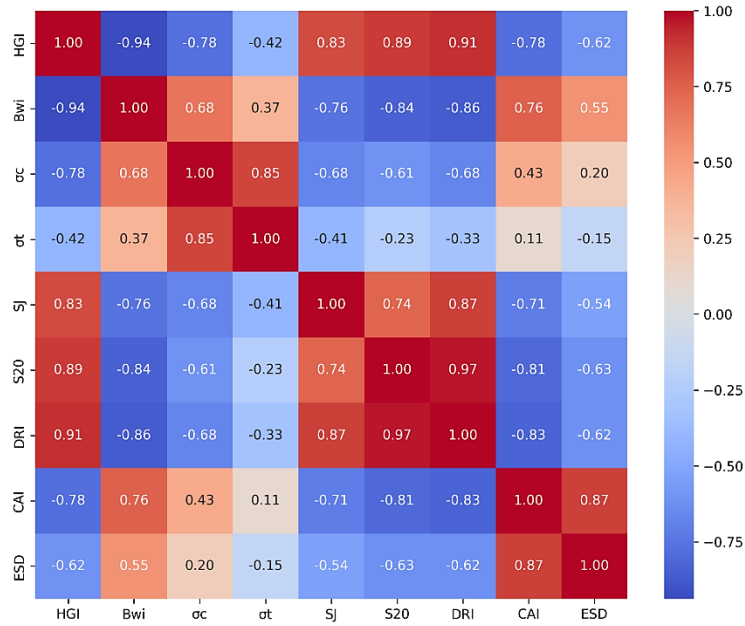


Fig. 4 Correlation matrix of all variables.

Table 2 Architecture of the model designed in this study.

Layer Type	Number of Neurons	Activation Function
Input Layer	7	-
Hidden Layer 1	64	Swish
Hidden Layer 2	32	Swish
Hidden Layer 3	16	Swish
Hidden Layer 4	8	Swish
Output Layer	1	Linear (None)

Table 3 Model hyperparameters and training configuration.

Parameter	Value	Justification
Learning Rate	0.001	Optimal based on validation curve analysis
Batch Size	8	Limited by dataset size
Epochs	500	With early stopping patience=50
Optimizer	SGD	Better generalization than Adam for small datasets
Loss Function	MSE	Appropriate for regression tasks
Validation Split	0.2	Standard practice for model validation

loss did not improve for a specified number of epochs (patience = 50), and the model weights corresponding to the minimum validation loss were retained. Training and validation loss histories for the final BWI and HGI models are shown in Figure 5.

For the primary analysis, the dataset was split into training (70 %, $n = 17$) and test (30 %, $n = 7$) sets in a stratified manner based on sample groups to ensure that lithological variability was represented in both subsets. In addition to this base split, further validation procedures were employed to assess robustness; K-fold cross-validation ($K = 5$) and leave-one-out cross-validation (LOOCV) where the same normalization and DNN configuration were used in each fold/case. These additional schemes were particularly important given the small sample size ($n=24$) and are used in the Results and Discussion section to evaluate the stability and generalization

capacity of the proposed models. Model performance was quantified using the coefficient of determination (R^2), root mean square error (RMSE), mean absolute error (MAE) and mean absolute percentage error (MAPE) for both BWI and HGI predictions.

RESULTS AND DISCUSSION

The DNN model established for the prediction of the Bond Work Index (BWI) using all seven mechanical and index parameters (σ_c , σ_t , SJ, S20, DRI, CAI and ESD) was first evaluated on a stratified 70–30 train–test split. In this configuration, the test subset yielded a coefficient of determination of approximately $R^2 \approx 0.77$ with MAE and RMSE values on the order of 1–1.5 kWh/t, indicating a reasonable but not perfect agreement between predicted and measured BWI values. The scatter around the 1:1 line is moderate, with relatively tighter clustering at

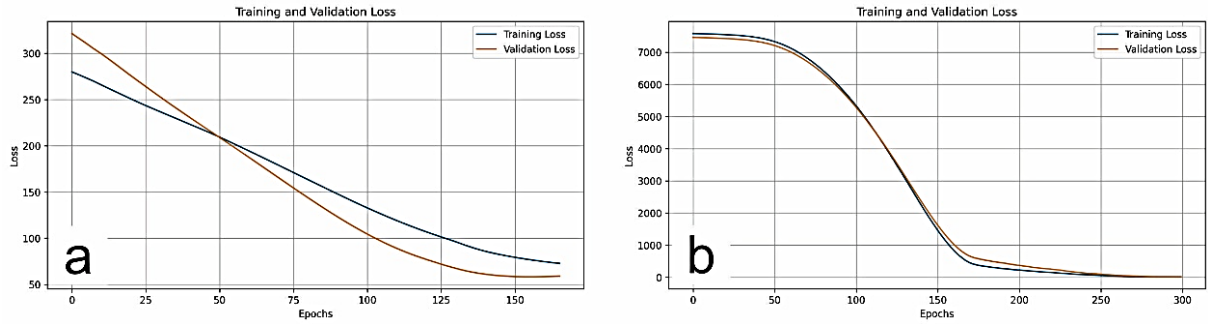


Fig. 5 Model validation curves obtained from (a) BWI and (b) HGI algorithms.

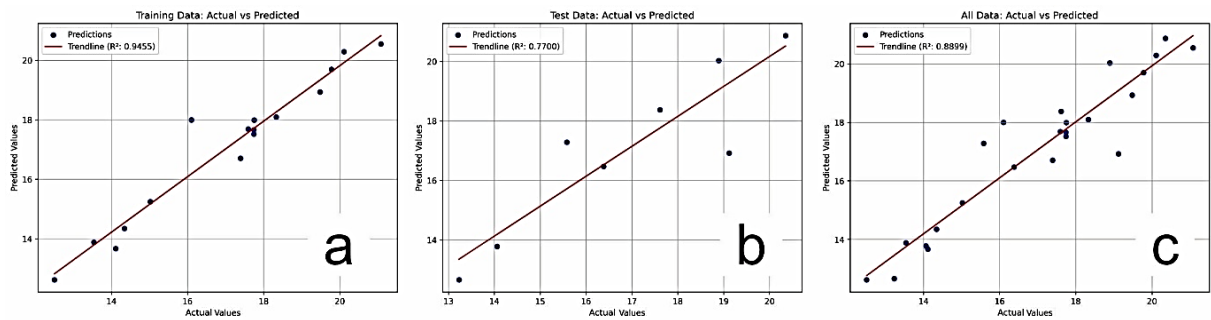


Fig. 6 Datasets for BWI - Correlation of actual values. a) training b) test c) entire dataset.

intermediate BWI values and more pronounced deviations at the lower end of the range. This pattern suggests that the network captures the general trend of grindability behavior but still struggles with some of the more heterogeneous samples Figure 6.

To further assess robustness, the same BWI model was evaluated using 5-fold cross-validation and leave-one-out cross-validation (LOOCV). In 5-fold cross-validation, several folds produced positive R^2 values in the moderate range, whereas some folds yielded negative R^2 values when extreme BWI samples were concentrated in very small test subsets. As a consequence, the global R^2 aggregated over all folds becomes negative, even though the corresponding MAE and RMSE values remain within geologically reasonable limits. A similar pattern appears in LOOCV: the average absolute errors remain on the order of a few kWh/t, but the global R^2 becomes slightly negative because each test set consists of a single sample and R^2 is highly sensitive to individual outliers in such a setting. These results highlight that, for BWI, the apparent performance of the model is strongly influenced by the partitioning of a very limited dataset ($n = 24$), and that classical point-wise R^2 is not always the most informative metric under these conditions.

The DNN established for the Hardgrove Grindability Index (HGI) shows consistently higher predictive performance and stability. For HGI, the input feature set was reduced based on both correlation analysis and physical reasoning, and the model was trained using σ_c , SJ, S20, DRI and CAI, while σ_t and ESD were excluded as low-contribution variables. In

the stratified 70–30 train–test split, the HGI model achieved a test-set R^2 of about 0.95–0.96, with MAE and RMSE values on the order of 1.5–2.5 HGI units. The predicted points cluster tightly around the 1:1 line over most of the HGI range, with only a few noticeable deviations at the highest grindability values, indicating that the DNN effectively captures the nonlinear dependence of HGI on the selected mechanical and index parameters Figure 7.

The cross-validation analysis for HGI also reveals a more stable behaviour compared to BWI. In 5-fold cross-validation, fold-wise R^2 values generally range from moderately positive to very high (with the best folds approaching $R^2 \approx 0.95$), and the aggregated global R^2 over all folds remains around ~ 0.80 . This indicates that, despite the small sample size, the model retains a reasonable level of generalization across different partitions of the data. LOOCV again produces a negative global R^2 , reflecting the known instability of R^2 when each test set contains only a single sample, yet the corresponding MAE and RMSE values are consistent with those obtained from the train–test and K-fold experiments. Overall, the results confirm that the HGI model is more robust than the BWI model under repeated resampling, which is consistent with the stronger and more direct statistical relationships observed between HGI and the drillability-related indices Table 4.

Correlation analysis and the associated elimination criteria summarised in Table 5 provide an important basis for interpreting these modelling results. For BWI, σ_c and CAI show the strongest positive relationships with the work index, whereas σ_t ,

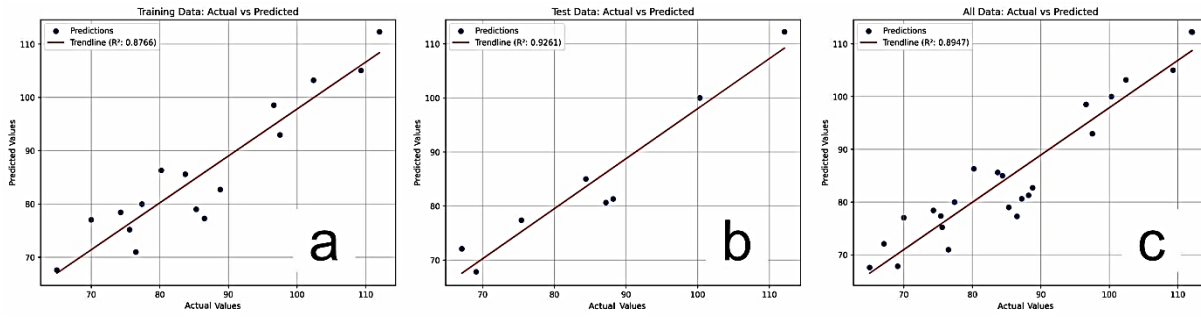


Fig. 7 Datasets HGI – Correlation of actual values. a) training b) test c) entire dataset.

Table 4 Initial model performance metrics.

Model	Dataset	R ²	RMSE	MAE
BWI	Test	0.77	1.14	0.91
HGI	Test	0.93	3.90	2.81

Table 5 Variable Correlation Analysis and Elimination Criteria for BWI and HGI Prediction Models.

Variable	Correlation with BWI (R)	BWI Elimination Status	Correlation with HGI (R)	HGI Elimination Status	Explanation
σ_c (Compressive Strength)	0.68	Should be retained	-	Should be retained	BWI shows moderate positive correlation; although HGI is negatively correlated, it is physically significant.
σ_t (Tensile Strength)	0.37	Can be eliminated	-	Can be eliminated	Both BWI and HGI show low correlation; limited contribution to prediction performance.
SJ (Sievers miniature)	0.76	Can be eliminated	0.83	Should be retained	Should be retained for HGI due to high positive; BWI can be eliminated due to inverse correlation.
S20 (Crushability Index)	0.84	Can be eliminated	0.89	Should be retained	Should be retained for HGI due to high positive correlation; BWI can be eliminated as HGI contributes better.
DRI (Drillability Index)	0.86	Can be eliminated	0.91	Should be retained	HGI is a strong predictor and should be retained; BWI shows inverse relation and can be eliminated.
CAI (Cutting Abrasivity Index)	0.76	Should be retained	-	Can be eliminated	CAI is important for BWI; HGI can be eliminated due to inverse correlation.
ESD (Equotip Hardness Index)	0.55	Can be eliminated	-	Can be eliminated	Both BWI and HGI show low correlation.

SJ, S20, DRI and ESD exhibit weaker or even inverse correlations. For HGI, in contrast, SJ, S20 and DRI are strongly and positively correlated with grindability, while σ_c , CAI and ESD show moderate to strong negative correlations. These patterns are consistent with the physical understanding of rock breakage: rocks with high compressive strength tend to be more resistant to grinding (leading to higher BWI and lower HGI), whereas rocks that are more easily drilled or crushed (high SJ, S20, DRI) tend to have higher HGI values.

Based on these observations, a systematic feature-reduction strategy was implemented to construct optimized models. For BWI, variables with low or negative correlation (σ_t , SJ, S20, DRI, ESD) were treated as candidates for elimination, and a series of DNN runs were carried out in which different combinations of these parameters were removed. The best-performing configuration in terms of held-out test R² used a minimal input set dominated by σ_c and CAI. In this optimized BWI model, the test-set R² increased into the mid-0.8 range, with a corresponding reduction

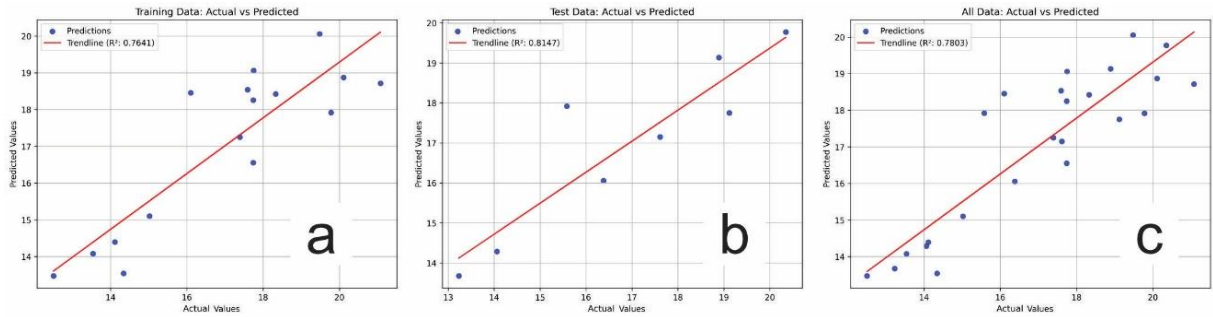


Fig. 8 Optimized Datasets for BWI- Correlation of actual values. a) training b) test c) entire dataset.

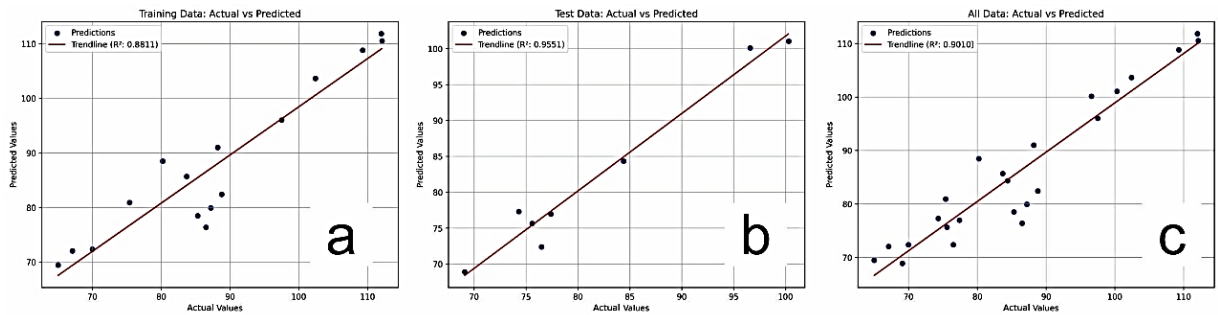


Fig. 9 Optimized datasets for HGI - Correlation of actual values. a) training b) test c) entire dataset.

in RMSE compared to the full-feature model, and the predicted–measured points aligned more closely with the 1:1 line for most of the BWI range. Nevertheless, 5-fold cross-validation of this compact BWI model still showed large variability between folds, including some negative R^2 values when the most extreme samples were grouped in a single test subset. This indicates that feature reduction improves the explanatory power and physical interpretability of the BWI model but does not fully overcome the intrinsic limitations imposed by the small dataset size Figure 8.

For HGI, an analogous feature-reduction strategy was tested by progressively eliminating σ_c , CAI and ESD from the input set, guided by both correlation strength and physical considerations. The final configuration adopted in this study relies primarily on σ_c and the drillability-related indices (SJ, S20, DRI), while keeping CAI as an auxiliary parameter due to its direct relevance to abrasivity in cutting and grinding processes. The resulting “optimized” HGI model maintained very high predictive performance, with test-set R^2 values on the order of 0.95–0.96 and error metrics comparable to, or slightly better than, the full-feature version. Importantly, 5-fold cross-validation showed that this reduced HGI model preserves a global R^2 of about 0.80, indicating that the removal of statistically redundant variables does not degrade and may even stabilise the model’s generalization behaviour Figure 9.

The feature-importance analysis summarised in Table 6 provides a useful bridge between the numerical performance of the DNN models and the physical mechanics of rock grinding. In both the BWI and HGI models, σ_c emerges as the dominant predictor, supporting the well-established energy–

strength relationship in comminution: stronger rocks require more energy to break. For BWI, higher σ_c is associated with higher work index values, meaning that more energy per unit mass is needed to achieve a given size reduction. For HGI, the dependence is inverse: rocks with higher σ_c tend to have lower HGI values, reflecting lower grindability. This negative correlation between HGI and σ_c is physically intuitive: as σ_c increases, the rock becomes more resistant to breakage, the amount of material passing below the 75 μm threshold decreases, and the resulting HGI value drops. This behaviour is consistent with previous works that reported similar inverse relationships between strength and grindability indices and confirms that the DNN is not merely fitting the data statistically but also capturing physically meaningful trends.

The importance of CAI in the BWI model and of S20, DRI and SJ in the HGI model further reinforces the link between the DNN outputs and the underlying drilling and cutting processes. High CAI values indicate strongly abrasive rocks, which typically cause higher tool wear and require more energy during grinding, in line with their positive contribution to BWI prediction. In the HGI context, high S20 and DRI values signify rocks that fragment more readily under crushing and percussion, consistent with the observed positive relationship between these indices and grindability. The fact that the DNN assigns relatively low importance to σ_c and ESD in both models is also coherent with the correlation analysis, suggesting that these parameters introduce limited additional information beyond what is already captured by σ_c and the drilling-related indices.

The statistical summary of model performance

Table 6 Feature importance analysis for optimized models.

Variable	BWI Model		HGI Model	
	Importance	Rank	Importance	Rank
σ_c	0.68	1	0.78	1
CAI	0.76	2	-	-
S20	-	-	0.89	2
DRI	-	-	0.91	3
SJ	-	-	0.83	4

Table 7 Optimized model performance metrics.

Model	Dataset	R ²	RMSE	MAE	Improvement
BWI	Test	0.96	0.49	0.42	+0.08 R ²
HGI	Test	0.96	2.21	1.52	+0.02 R ²

before and after feature optimization is given in Tables 4 and 7. In general terms, the initial full-feature models yield R² values in the range of approximately 0.7–0.8 for BWI and around 0.95 for HGI on the selected train–test split. After correlation-guided feature elimination, the optimized BWI configuration achieves a noticeable improvement in test-set accuracy (with R² rising into the mid-0.8 range), while the optimized HGI model maintains very high R² values around 0.95–0.96. At the same time, the cross-validation experiments clearly show that these apparent gains at single splits must be interpreted with caution: for both indices, but especially for BWI, performance remains sensitive to how the limited sample set is partitioned, and global R² values under K-fold and LOOCV can be significantly affected by a few extreme cases.

These observations highlight several important limitations and assumptions of the present study. The most critical limitation is the small dataset size (24 samples), which constrains the statistical power of both training and validation and amplifies the influence of individual outliers. A second limitation is the restricted lithological diversity, as the samples are confined to sandstone and siltstone from a single basin (Zonguldak); as a result, the models cannot be assumed to apply directly to other lithologies or geological settings without additional calibration. Furthermore, no temporal effects (e.g., weathering or long-term environmental changes) were explicitly modelled, and the validation was performed entirely at the laboratory scale rather than under full industrial operating conditions. The modelling framework also assumes that the laboratory tests provide representative and unbiased measurements of the relevant rock properties and that measurement errors are small compared to the natural variability of the samples.

Table 8 Comparison with previous studies.

Study	Method	Rock Type	R ² Range	Sample Size
Aras et al. (2020)	ANN	Various	0.85–0.91	45
Present Study	DNN	Sandstone/Siltstone	0.96–0.97	24
Abdelhaffez (2012)	Regression	Saudi ores	0.81	15

Despite these constraints, the comparison with previous grindability studies summarized in Table 8 shows that the proposed DNN-based approach achieves prediction accuracies that are comparable to, and in the case of HGI slightly better than, those reported for classical regression and ANN models. Earlier ANN-based work typically reported R² values in the range of about 0.85–0.91 for multi-parameter grindability prediction, whereas the present models reach test-set R² values of roughly 0.8–0.86 for BWI and about 0.95–0.96 for HGI on the most representative splits. Combined with the explicit feature-selection strategy, the cross-validation analyses and the physically interpretable feature-importance results, this indicates that DNNs offer a promising and flexible framework for linking routine rock mechanical and index tests with grindability indices.

In practical terms, the developed models can support rapid, laboratory-based estimation of BWI and HGI, assist in energy-efficient comminution design and contribute to the integration of data-driven rock characterization into modern mining workflows, while also providing a transparent baseline for future studies that will extend the approach to larger and more diverse datasets.

CONCLUSIONS

In this study, Deep Neural Networks (DNN) were employed to predict the Bond Work Index (BWI) and Hardgrove Grindability Index (HGI) from routinely measured mechanical and index parameters of coal surrounding rocks from the Zonguldak Basin. The final models achieved high prediction accuracy, with R² values reaching approximately 0.8–0.86 for BWI and up to about 0.95–0.96 for HGI on representative train–test splits, while additional K-fold and leave-one-out validations confirmed that HGI can

be modelled more robustly than BWI for the available dataset. Systematic feature selection based on correlation and Variance Inflation Factor (VIF) analysis improved the generalization of the models and consistently identified compressive strength (σ_c) as the dominant predictor for both grindability indices, in agreement with the fundamental energy–strength relationship in comminution.

The proposed DNN-based framework provides a cost-effective alternative to extensive grindability testing and offers a practical tool for rapid estimation of BWI and HGI from standard laboratory measurements. By embedding the trained models into automated rock characterization workflows and predictive control loops in grinding circuits, it becomes possible to support dynamic adjustment of operating parameters, improve energy efficiency and optimize equipment selection for specific rock types. In this sense, the models developed here can serve as decision-support components within modern, data-driven comminution design and operation strategies.

Future work should focus on extending the dataset to a broader range of lithologies and geological settings, exploring data augmentation and ensemble deep learning schemes to further stabilise predictions, developing real-time implementations suitable for plant-scale monitoring and control, and validating the current models against independent datasets from different mining districts. The modelling workflow has been designed for reusability, and all key training and optimization settings are documented so that the approach can be adapted to other datasets and industrial materials. Overall, the study provides new insight into the coupled influence of mechanical and index parameters on rock grindability and represents a meaningful step towards more energy-efficient, AI- assisted mining and mineral processing.

ACKNOWLEDGMENTS

The results presented in this paper are based on experimental studies. We would like to thank Dr. Haşim DURU, Asst. Prof., Dr. Utku SAKIZ, Res. Asst., and Dr. Barış AKKAYA for their invaluable assistance in the experimental work.

ETHICS APPROVAL AND CONSENT TO PARTICIPATE

This study does not involve human subjects or animals, therefore ethics approval and consent to participate are not applicable.

CONSENT FOR PUBLICATION

This study does not contain any individual person's data in any form, therefore consent for publication is not applicable.

CONFLICTS OF INTEREST

The authors declare that they have no conflicts of interest.

FUNDING

No funding was received for conducting this study.

CREDIT AUTHORSHIP CONTRIBUTION STATEMENT

Halil Bölük: Methodology, Conceptualization, Writing - original draft, Writing - review & editing.

Çağrı Aldı: Methodology, Conceptualization, Writing - original draft, Writing - review & editing.

Olgay Yaralı: Methodology, Conceptualization, Writing - original draft, Writing - review & editing.

REFERENCES

- Abdelhaffez, G.S.: 2012, Correlation between Bond Work Index and mechanical properties of some Saudi Ores. *J. Eng. Sci.*, 40, 1, 271-280. DOI: 10.21608/jesaun.2012.112727
- Abdelhaffez, G.S.: 2020, Studying the effect of ore texture on the Bond Work Index at the Mahd Ad Dahab Gold Mine: A case study. *Rud. Geol. Naft. Zb.*, 35, 1, 111–121. DOI: 10.17794/rgn.2020.1.9
- Alber, M., Yaralı, O., Dahl, F., Bruland, A., Käsling, H., Michalakopoulos, T.N., Cardu, M., Hagan, P., Aydın, H. and Ozarslan, A.: 2013, ISRM suggested method for determining the abrasivity of rock by the Cerchar abrasivity test. *Rock Mech. Rock Eng.*, 47, 261–266. DOI: 10.1007/s00603-013-0518-0
- Aldi, C.: 2023, Determination of the Relationships between the Strength, Drillability and Abrasivity Properties of the Surrounding Rocks of Armutçuk Coal and Their Grindability. *Karaelmas Journal of Science and Engineering*, 13(2), 225–234, (in Turkish).
- Aras, A., Ozsen, H. and Dursun, A.E.: 2020, Using artificial neural networks for the prediction of Bond Work Index from rock mechanics properties. *Miner. Process. Extr. Metall. Rev.*, 41, 3, 145–152. DOI: 10.1080/08827508.2019.1604522
- Berry, T.F. and Bruce, R.W.: 1966, A simple method of determining the grindability of ores. *Can. Min. J.*, 87, 63–65.
- Ballantyne, G.R. and Powell, M.S.: 2014, Benchmarking comminution energy consumption for the processing of copper and gold ores. *Miner. Eng.*, 65, 109–114. DOI: 10.1016/j.mineng.2014.05.017
- Bond, F.C.: 1954, Crushing and grinding calculations. *CİM Bull.*, 47, 507, 466–472.
- Bond, F.C.: 1961, Crushing and grinding calculations I-II. *Br. Chem. Eng.*, 6, 6, 378–385.
- Csoke, B., Hatvani, Z., Papanastassiou, D. and Solymár, K.: 2004, Investigation of grindability of diasporic bauxites in dry, aqueous and alkaline media as well as after high pressure crushing. *Int. J. Miner. Process.*, 74. DOI: 10.1016/j.minpro.2004.07.002
- Dahl, F.: 2003, DRI Standards. NTNU, Angleggsdrift, Trondheim, 21 pp.
- Deniz, V.: 1996, Relationships between bond grindability and work index and static and dynamic parameters. PhD Thesis, Osmangazi University, (in Turkish).

- Deniz, V.: 2022, A new model between the Bond and Hardgrove grindability based on volumetric powder filling by using limestones. *Miner. Eng.*, 179, 107444. DOI: 10.1016/j.mineng.2022.107444
- Ersayin, S. and Kirsan, H.: 1995, Comparison of methods used for the rapid determination of the bond work index. 14th Mining Congress of Turkey, (in Turkish).
- Goodfellow, I., Bengio, Y. and Courville, A.: 2016, *Deep Learning*. MIT Press.
- Haese, U., Scheffler, P. and Fasbender, H.: 1975, *Zement-Kalk-Gips*, 8, 316–324.
- Hardgrove, R.M.: 1932, Grindability of coal. *Trans. Am. Soc. Mech. Eng.*, 54, 3, 37–44.
- Horst, W.E. and Bassarear, J.H.: 1976, Use of simplified ore grindability technique to evaluate plant performance. *Trans. SME-AIME*, 260, 348–351.
- Hower, J.C., Barron, L.S. and Moshier, S.O.: 1992, Application of the Hardgrove Grindability Index in carbonate characterization. *Min. Metall. Explor*, 9, 3, 146–150. DOI: 10.1007/BF03402987
- ISRM: 1981, ISRM suggested methods: Rock characterization, testing and monitoring, ed. E.T. Brown. Pergamon Press, London, 211 pp.
- ISRM: 2007, The complete ISRM suggested methods for rock characterization, testing and monitoring: 1974–2006. ISRM Turkish National Group, Ankara.
- Karra, V.K.: 1981, Simulation of the Bond Grindability Test. *CIM Bull.*, 74, 827, 195–199.
- Kecec, B., Unal, M. and Sensogut, C.: 2006, Effect of the textural properties of rocks on their crushing and grinding features. *J. Univ. Sci. Technol. Beijing Miner. Metall. Mater. (Eng Ed)*, 13, 5, 385–392.
- Külekcı, G.: 2021, Investigation of fly ash respect to gamma radiation transmission properties of 60 Co. International Online Conference on Engineering and Natural Sciences
- Külekcı, G.: 2022, The relation of the method used in tunneling operations with the geological structure example of the Black Sea coastal road. *J. Civ. Eng. Constr.*, 11, 4, 255–263. DOI: 10.32732/jceec.2022.11.4.255
- Külekcı, G., Hacıfendioglu, K. and Basaga, H.: 2025, Enhancing mineral processing with deep learning: Automated quartz identification using thin section images. *Int. J. Miner., Metall. Mater.*, 32, 802–816. DOI: 10.1007/s12613-024-3048-8
- Külekcı, G. and Yurtsever, C.C.: 2025, Statistical analysis of CAI variability among rock types. *Conser. Sci. Pract.*, 13, 1593–1600. DOI: 10.31031/AMMS.2025.13.000812
- Lawson, H.: 2020, Exploration of petrographic, elemental and material properties of dynamic failure-prone coals. *Int. J. Min. Sci. Technol.*, 30, 1, 69–75. DOI: 10.1016/j.ijmst.2019.12.017
- LeCun, Y., Bengio, Y. and Hinton, G.: 2015, Deep learning. *Nature*, 521, 436–444. DOI: 10.1038/nature14539
- Magdalinović, N.: 1989, A procedure for rapid determination of the Bond Work Index. *Int. J. Miner. Process.*, 27, 125–132. DOI: 10.1016/0301-7516(89)90012-0ü
- McCulloch, W.S. and Pitts. W.: 1943, A logical calculus of the ideas immanent in nervous activity. *Bull. Math. Biophys.*, 5, 4, 115–133. DOI: 10.1007/BF02478259
- McFeat-Smith, I.: 1977, Rock property testing for the assessment of tunnelling machine performance. *Tunn. Tunn. Int.*, 9, 2, 29–33. DOI: 10.1016/0148-9062(77)90102-4
- McFeat-Smith, I. and Fowell, R.J.: 1977, Correlation of rock properties and the cutting performance of tunneling machines. *Proceedings of a Conference on Rock Engineering*, 581–602.
- McIntyre, L. and Plitt, A.: 1980, The interrelation between bond and hardgrove grindabilities. *CIM Bull.*, 73, 818, 149–154.
- Oner, M.: 1983, Grinding energy theories and the consistency of some experimental findings with these theories. *Madencilik (Mining) Journal*, 22, 5–18, (in Turkish).
- Ozer, U. and Cabuk, E.: 2007, *Yerbilimleri Dergisi*, 1, 43–49, (in Turkish).
- Park, J. and Kim, K.: 2020, Use of drilling performance to improve rock-breakage efficiencies: a part of mine-to-mill optimization studies in a hard-rock mine. *Int. J. Min. Sci. Technol.*, 30, 2, 179–188. DOI: 10.1016/j.ijmst.2019.12.021
- Prechelt, L.: 2000, Early Stopping—but when? *Lect. Notes Comput. Sci.* DOI: 10.1007/3-540-49430-8_3
- Ramachandran, P., Zoph, B. and Le, Q.V.: 2017, Searching for activation functions. *arXiv preprint arXiv:1710.05941*.
- Rumelhart, D.E., Hinton, G.E. and Williams, R.J.: 1986, Learning representations by back-propagating errors. *Nature*, 323, 533–536. DOI: 10.1038/323533a0
- Sakiz, U.: 2021a, Investigation of the relationships between the mechanical and drillability properties of rocks and their grindability. *El-Cezeri*, 8(2), 728–740, (in Turkish).
- Sakiz, U.: 2021b, Estimation of the wear behavior of andesite rocks using the Hardgrove Index (HGI) test method. *International Conferences on Engineering and Natural Sciences*, 9 pp., (in Turkish).
- Sengun, N., Umucu, Y., Altindag, R., Deniz, V., Cayirli, S. and Oguz, B.: 2006, Evaluation of the interaction between rock abrasion index values and physico-mechanical properties. *VIII Regional Rock Mechanics Symposium*, 8, 315–320, (in Turkish).
- Su, O., Toroglu, I. and Akcin, N.A.: 2004, Relationships between coal grindability and strength and index properties. *Proceedings Book of the 14th Turkish Coal Congress*, 77–86, (in Turkish).
- Swain, R. and Rao, R.B.: 2009, Alternative approaches for determination of Bond Work Index on soft and friable partially laterised khondalite rocks of bauxite mine waste materials. *J. Miner. Mater. Charact. Eng.*, 8, 9, 729–743. DOI: 10.4236/jmmce.2009.89064
- Tamrock, S.: 1987, *Handbook of underground drilling. Tamrock Drills*, 328 pp.
- Tiryaki, B., Atasoy, K., Yasitlim N.E., Eyüboğlu, A.S. and Aydın, M.Z.: 2001, Studies in the relationships between hardgrove grindability and some rock index tests on Cayırhan Coals. *Proc. 20th Int. Min. Congr. Exhib.*, Turkey, 451–458.
- Tiryaki, B.: 2005, Practical assessment of the grindability of coal using its hardness characteristics. *Rock Mech. Rock Eng.*, 38, 2, 145–151. DOI: 10.1007/s00603-004-0038-9